


# Extracellular microRNA 130b-3p inhibits eCIRP-induced inflammation

Steven D Gurien<sup>1,2</sup>, Monowar Aziz<sup>1</sup>, Hui Jin<sup>1</sup>, Haichao Wang<sup>3</sup>, Mingzhu He<sup>4</sup>, Yousef Al-Abed<sup>4</sup>, Jeffrey M Nicastro<sup>2</sup>, Gene F Coppa<sup>2</sup> & Ping Wang<sup>1,2\*</sup> 

## Abstract

Although microRNAs regulate mRNA expression intracellularly, they are often released into the circulation in inflammatory diseases. During sepsis, secreted extracellular cold-inducible RNA-binding protein (eCIRP) acts as a damage-associated molecular pattern (DAMP), inducing tissue damage by elevating inflammatory cytokines and chemokines. Here, we report that the circulating microRNA 130b-3p inhibits eCIRP-mediated sterile and cecal ligation and puncture (CLP)-induced non-sterile inflammation. We find that levels of miR-130b-3p are increased in the serum of septic mice and patients and that it strongly interacts with recombinant murine (rm) CIRP *in vitro* and with eCIRP in the serum of septic mice *in vivo*. Combining a miR-130b-3p mimic with rmCIRP significantly decreases TNF- $\alpha$  release by macrophages compared to only rmCIRP-treated cells. This combined treatment also dose-dependently decreases the affinity of rmCIRP with its receptor TLR4/MD2. Finally, injection of a miR-130b-3p mimic significantly reduces rmCIRP- or CLP-induced systemic inflammation and acute lung injury in mice. These data show that extracellular miR-130b-3p functions as a novel endogenous inhibitor of eCIRP and point to an innovative therapeutic approach to treat inflammatory diseases.

**Keywords** eCIRP; inflammation; macrophages; miRNA 130b-3p; sepsis

**Subject Categories** Immunology; RNA Biology

**DOI** 10.15252/embr.201948075 | Received 12 March 2019 | Revised 18 October 2019 | Accepted 24 October 2019 | Published online 14 November 2019

**EMBO Reports (2020) 21: e48075**

See also: **K Van Looveren et al** (January 2020)

## Introduction

Inflammation occurs from the activation of the immune cells particularly macrophages by pathogen-associated molecular patterns (PAMPs) or damage-associated molecular patterns (DAMPs) [1]. Sepsis, trauma, hemorrhage, and ischemia–reperfusion (I/R) lead to

the release of DAMPs and subsequently cause inflammation [1,2]. DAMPs include but are not limited to high-mobility group box 1 (HMGB1), mitochondrial DNA, and cellular chaperones (e.g., heat shock proteins) [3]. Toll-like receptors (TLRs) are located both intracellularly and on the cell surface of macrophages. These receptors respond to several different PAMPs and DAMPs [3–5], and transduce an intracellular signal, leading to the activation of nuclear factor- $\kappa$ B (NF- $\kappa$ B) and other inflammatory pathways [5].

Cold-inducible RNA-binding protein (CIRP) is a small 172-amino-acid RNA chaperone protein [6] and is secreted into the extracellular space in inflammatory diseases such as sepsis, I/R injuries, and hemorrhagic shock (reviewed in [7]). Extracellular CIRP (eCIRP) acts as a DAMP which causes inflammation and tissue damage via elevating inflammatory cytokines and chemokines [7]. eCIRP accomplishes this by binding to the TLR4 and myeloid differentiation factor 2 (MD2) complex on macrophages, leading to the activation of NF- $\kappa$ B [8,9]. This causes the downstream effect of elevated levels of tumor necrosis factor- $\alpha$  (TNF- $\alpha$ ), interleukin-6 (IL-6), HMGB1, and IL-1 $\beta$  [7–9].

MicroRNAs (miRNAs) are short RNA molecules approximately 22 base pairs long [10]. They are transcribed in the nucleus as primary miRNAs. After several modifications occurring in both the nucleus and the cytoplasm, primary miRNAs become double-stranded miRNAs. The lead strand is then loaded onto an Argonaute protein to form an RNA-induced silencing complex (RISC), while the passenger strand is lost [10,11]. RISC then binds to and inhibits the translation of specific mRNAs, usually by making them unstable and creating a shorter half-life. Since binding does not require perfect complementary between the mRNA and the miRNA, each miRNA may bind several hundred different types of mRNAs [12].

While the physiological role of miRNAs has mostly been found to occur intracellularly, miRNAs have also been identified in the extracellular space [13]. They are surprisingly stable in the blood and can be measured in plasma [14,15]. This has prompted many studies to look into the efficacy of using extracellular miRNAs as diagnostic and prognostic markers for different diseases such as sepsis, cancers, and autoimmune diseases [16–18]. The precise role of extracellular miRNA has yet to be adequately understood. A recent study demonstrated that treatment of mice and macrophages

1 Center for Immunology and Inflammation, The Feinstein Institutes for Medical Research, Manhasset, NY, USA

2 Department of Surgery, Donald and Barbara Zucker School of Medicine at Hofstra/Northwell, Manhasset, NY, USA

3 Center for Biomedical Science, The Feinstein Institutes for Medical Research, Manhasset, NY, USA

4 Center for Molecular Innovation, The Feinstein Institutes for Medical Research, Manhasset, NY, USA

\*Corresponding author. Tel: +1 516 562 3411; Fax: +1 516 562 2396; E-mail: pwang@northwell.edu

with selected extracellular miRNA mimics induced the expression of pro-inflammatory cytokines through a TLR7/MyD88-dependent pathway following their transfection into the cells [19]. During sepsis, eCIRP and certain extracellular miRNA levels both become elevated in the blood [8,17]. While it has been shown that RNA-binding protein CIRP interacts with nascent mRNA [6,7,20], the interaction between eCIRP and extracellular miRNA, and the impact of this extracellular interaction on immune cells has never been studied before. We therefore hypothesized that certain miRNAs released into the circulation can interact with eCIRP and regulate eCIRP's binding to TLR4. Out of the three miRNAs 130b-3p, 27b, and 140, we found that miRNA 130b-3p had the highest elevation in the serum during sepsis, the strongest binding affinity to eCIRP, and the highest inhibition of

eCIRP-induced inflammation via macrophages. Extracellular miRNA 130b-3p serves as a novel endogenous inhibitor of eCIRP, and thus potentially is a novel therapeutic tool in counteracting inflammation.

## Results

### Sepsis increases serum levels of miRNA 130b-3p

Our PCR array data revealed that several miRNAs linked to inflammatory pathways were increased in the serum of septic mice (Figs 1A and EV1, Table EV1). We found that miRNAs 130b-3p, 27b, and 140, which have all been highly implicated in

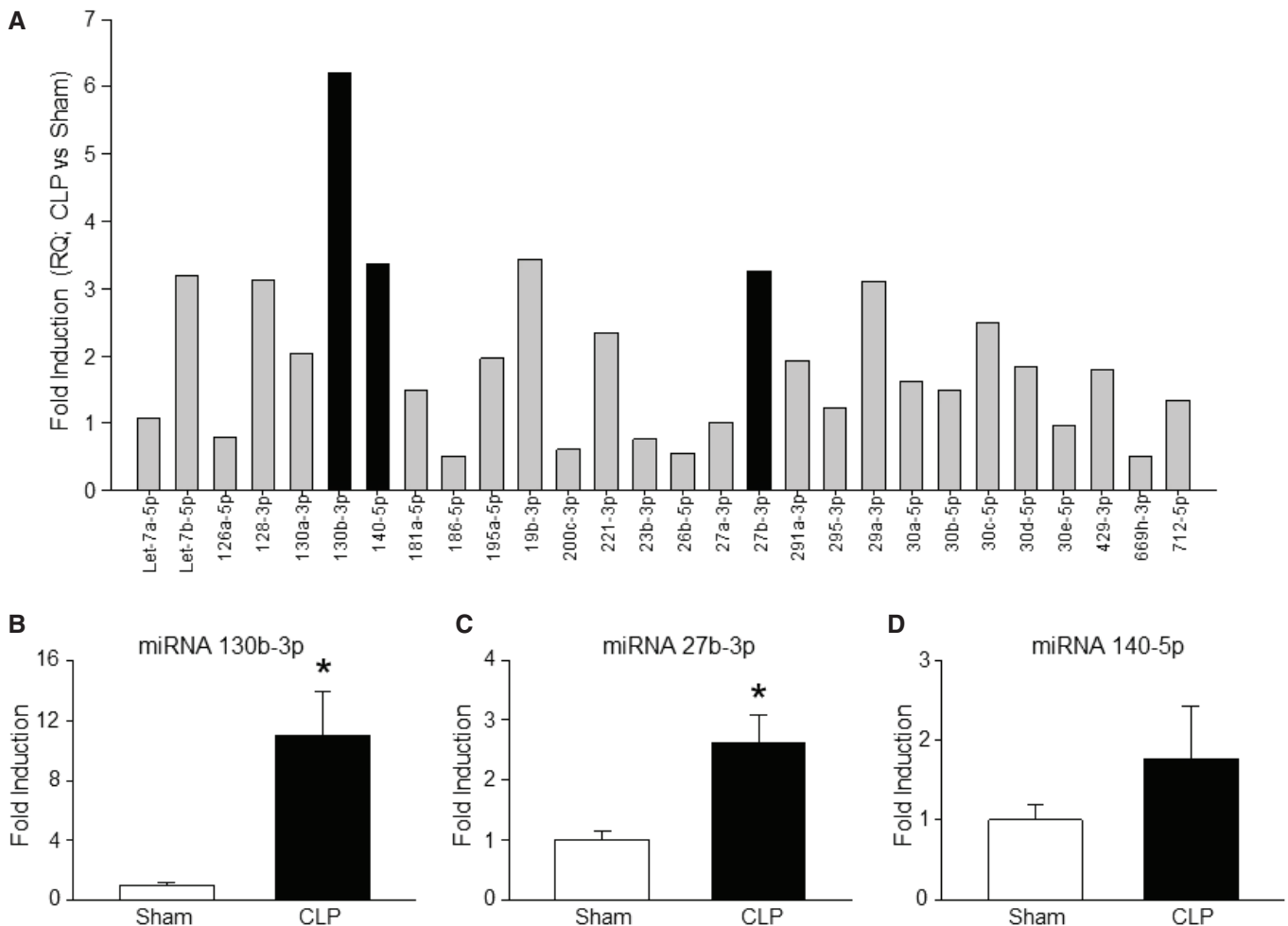


**Figure 1. MicroRNA 130b-3p is increased in the serum during sepsis.**

Mice either underwent CLP for 24 h, or underwent laparotomy alone with no CLP (sham mice). Blood samples were collected at 24 h and miRNA was extracted, which was then used for PCR array profiling using qRT-PCR.

A Bar diagram representing the fold increase in the levels of serum miRNAs of CLP vs. sham mouse obtained from inflammatory pathway-specific PCR array analysis ( $n = 1$  mouse/group) is shown. The cycle threshold (CT) values of serum miRNAs of sham and CLP mice are presented in Fig EV1. *Caenorhabditis elegans* miRNA 39-3p was spiked in and used to normalize comparative CT values (Table EV1). Relative quantities (fold induction) compared to sham mouse serum miRNAs were determined by using  $2^{-ddCT}$ .

B–D Validation of increased circulating (B) miRNA 130b-3p ( $n = 8$  mice/group), (C) miRNA 27b ( $n = 8$  mice/group), and (D) miRNA 140 ( $n = 8$  mice/group). *C. elegans* miRNA 39-3p was spiked in and used to normalize comparative CT values (Table EV2). Relative quantities (fold induction) compared to sham mouse serum miRNAs were determined by using  $2^{-ddCT}$ .

Data information: Data are expressed as means  $\pm$  SE and compared by Student's *t*-test. \* $P < 0.05$  vs. sham. CLP, cecal ligation and puncture.

inflammation [21–23], were markedly upregulated in the serum of septic mice (Fig 1A). Further confirmation by RT–qPCR in the upregulation of serum levels of miRNAs 130b-3p, 27b, and 140 of septic mice revealed that miRNA 130b-3p was significantly increased by  $11 \pm 3.2$ -fold compared to sham mice. By contrast, miRNA 27b and miRNA 140 had a fold increase in their serum levels by only  $2.6 \pm 0.4$  and  $1.8 \pm 0.6$ , respectively (Fig 1B–D; Table EV2). These data suggest that sepsis leads to an efflux of these three miRNAs into the circulation during sepsis, with miRNA 130b-3p having the greatest increase.

### Serum levels of miRNA 130b-3p and eCIRP are both increased in septic patients

Since our murine model of sepsis showed significantly increased levels of miRNA 130b-3p in the serum compared to sham mice (Fig 1A and B), we next aimed to determine the serum levels of miR130b-3p in healthy human subjects and septic patients. In order to do this study, we obtained de-identified serum samples from 15 septic patients and seven healthy individuals. Patient samples were obtained from the Department of Emergency Medicine, North Shore University Hospital, Manhasset, New York. We found that the levels of miR130b-3p in the serum of septic patients were markedly elevated by 2.4-fold compared to healthy individuals (Fig 2A, Table EV3). We assessed eCIRP levels in the serum of these patients and healthy controls and found that septic patients had significantly higher levels of eCIRP in their blood compared to healthy individuals (Fig 2B).

### miRNA 130b-3p has a strong binding affinity to CIRP and attenuates eCIRP's induction of pro-inflammatory cytokines in macrophages

Cold-inducible RNA-binding protein has an N-terminal RNA-binding domain [7,20]. However, whether or not eCIRP binds to miRNAs is unknown. To determine the possible binding of miRNAs to eCIRP, a BIAcore study was performed on the three miRNAs 130b-3p, 27b, and 140. We found that miRNA 130b-3p had the strongest binding affinity to rmCIRP with a  $K_d$  value of  $5.0 \times 10^{-8}$  M (Fig 3A). Although miRNA 27b and miRNA 140 had strong binding affinities to rmCIRP with  $K_d$  values of  $8.4 \times 10^{-8}$  and  $16 \times 10^{-8}$  M, respectively, they were 1.7 and 3.2 times weaker than miRNA 130b-3p's binding to rmCIRP (Fig 3B and C). Since rmCIRP binds to miRNAs 130b-3p, 27b, and 140, we therefore hypothesized that binding of rmCIRP with these miRNAs' mimics would alter rmCIRP's functional effects. We looked at TNF- $\alpha$  production of RAW264.7 macrophages when rmCIRP alone was added, and when rmCIRP was combined with one of the three miRNAs' mimics before being added to the cells. Treatment of RAW264.7 cells with rmCIRP alone dramatically increased TNF- $\alpha$  release (Fig 3D). Co-treatment of cells with rmCIRP and miRNA 140 mimic did not exert any inhibitory effect on TNF- $\alpha$  production, while miRNA 27b only had a mild inhibition (Fig 3D). Surprisingly, miRNA 130b-3p mimic displayed a significant inhibitory effect of rmCIRP-induced TNF- $\alpha$  release by 42% (Fig 3D). Since miRNAs 130b-3p, 140, and 27b are all recognized by eCIRP (Fig 3A–C), we next wanted to reveal whether or not the addition of miRNA 140 and 27b mimics along with miRNA 130b-3p mimic can enhance or attenuate the inhibitory effects miRNA 130b-3p mimic has

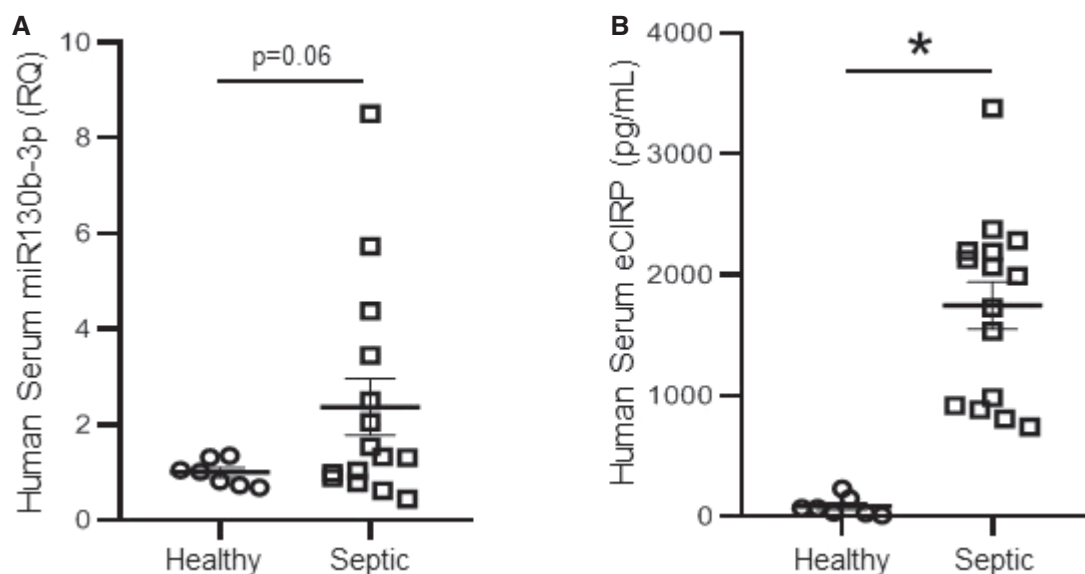


**Figure 2. Increased levels of miRNA 130b-3p and eCIRP in the serum of human septic patients.**

Total microRNA was extracted from the blood samples of healthy individuals and septic patients.

A miRNA 130b-3p expression in their serum samples was determined by qRT–PCR and represented in scatter plot. *Caenorhabditis elegans* miRNA 39-3p was spiked in and used to normalize comparative CT values (Table EV3). Relative quantities (fold induction) compared to healthy individuals' serum miRNAs were determined by using  $2^{-\Delta\Delta CT}$ .

B eCIRP levels were quantified in the serum samples of healthy controls and septic patients.

Data information: Data are expressed as means  $\pm$  SE and compared by Student's t-test ( $n = 7$  healthy control and 15 septic patients). \* $P < 0.05$  vs. healthy control. eCIRP, extracellular cold-inducible RNA-binding protein.

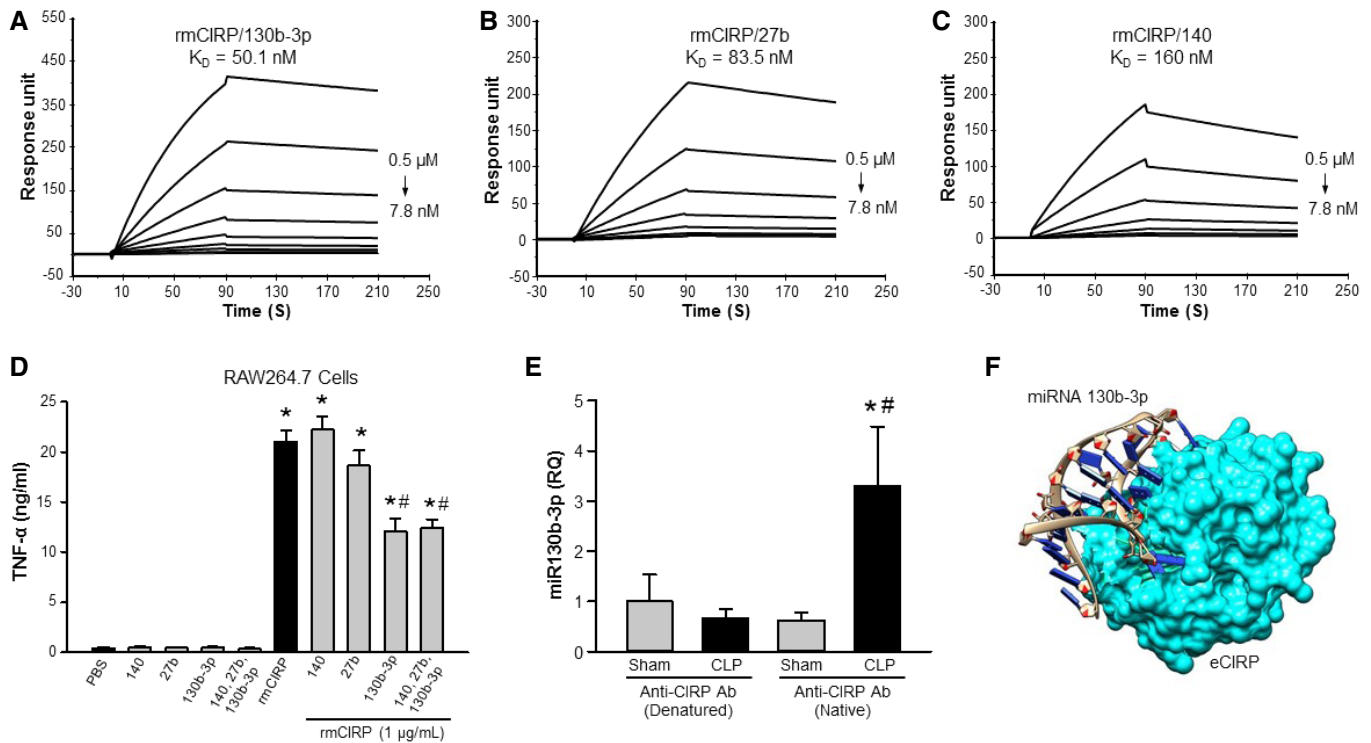


**Figure 3. MicroRNA 130b-3p exhibits the strongest binding affinity with rmCIRP and the highest TNF- $\alpha$  inhibition on RAW264.7 cells.**

A–C Biotinylated single-stranded forms of miRNAs 130b-3p, 27b, and 140 were individually immobilized on a sensor chip SA, and rmCIRP of varying concentrations was injected as the analyte. rmCIRP binds to (A) miRNA 130b-3p mimic with a  $K_d$  of  $50.1 \pm 3.0$  nM; (B) miRNA 27b mimic with a  $K_d$  of  $83.5 \pm 3.1$  nM; and (C) miRNA 140 mimic with a  $K_d$  of  $160 \pm 1.9$  nM. At least three ( $n = 3$ ) independent BIAcore experiments were performed.

D RAW264.7 cells ( $1 \times 10^6$  cells/ml) were stimulated with rmCIRP (1  $\mu$ g/ml) with and without each of the three miRNAs at a concentration of 100 nM or altogether with each at a concentration of 100 nM. The supernatant was collected at 24 h and assessed for TNF- $\alpha$  by ELISA.

E, F eCIRP binds to extracellular miRNA 130b-3p *in vivo*. Serum was isolated 20 h after CLP, or sham operation was performed on mice. Immunoprecipitation for eCIRP was then carried out on the serum by reacting the serum with either native CIRP Ab or denatured CIRP Ab. (E) All miRNAs were isolated from this IP, and miRNA 130b-3p was amplified with subsequent quantification using qPCR and compared to denatured CIRP Ab control ( $n = 6$  mice/group). *Caenorhabditis elegans* miRNA 39-3p was spiked in and used to normalize comparative CT values. Relative quantities (fold induction) compared to sham mouse serum miRNAs treated with denatured CIRP Ab were determined by using  $2^{-ddCT}$ . (F) Virtual modeling illustrating docking of miRNA 130b-3p and eCIRP. rmCIRP, recombinant murine cold-inducible RNA-binding protein.

Data information: Data are expressed as means  $\pm$  SE and compared by one-way ANOVA and SNK method ( $n = 6$  samples/group). (D)  $*P < 0.001$  vs. PBS,  $^{\#}P < 0.05$  vs. rmCIRP. (E)  $*P < 0.05$  vs. sham serum treated with denatured CIRP Ab and  $^{\#}P < 0.05$  vs. sham serum treated with native CIRP Ab.

on rmCIRP-mediated TNF- $\alpha$  production by macrophages. We found that there was no additional inhibition of rmCIRP-induced TNF- $\alpha$  or IL-6 production by the macrophages following treatment of cells with miR130b, 140, and 27b altogether compared to condition where only miR130b-3p mimic was added (Figs 3D and EV2). This implicated miRNA 130b-3p in having a functional role of inhibiting TNF- $\alpha$  production by macrophages after interacting with rmCIRP.

#### Extracellular miRNA 130b-3p binds to eCIRP *in vivo*

To determine whether extracellular miRNA 130b-3p and eCIRP interact *in vivo*, a co-immunoprecipitation (co-IP) experiment was carried out on the serum of sham and septic mice 20 h after CLP was performed. Either native form of CIRP Ab or denatured CIRP Ab as negative control was incubated with the serum before a magnetic co-IP was carried out. At the end of the co-IP, miRNA attached to the eCIRP was isolated and miRNA 130b-3p was quantified by real-time qPCR. As shown in Fig 3E, the RQ of eCIRP-bound miRNA 130b-3p of

the serum of sham and CLP mice following *ex vivo* treatment with denatured CIRP Ab was low and did not differ from each other. Surprisingly, the serum of CLP mice following *ex vivo* treatment with native CIRP Ab showed significant increase in the RQ of eCIRP-bound miRNA 130b-3p compared to sham mouse serum as well as to the serum of sham and CLP mice treated with denatured CIRP Ab (Fig 3E). These data clearly demonstrate eCIRP's binding to extracellular miRNA 130b-3p under *in vivo* condition and also suggest that the content of eCIRP-bound extracellular miRNA 130b-3p was dramatically increased during sepsis. Besides these *in vivo* findings, computational analysis illustrated the theoretical modeling of the two molecules docking (Fig 3F).

#### Dose response of miRNA 130b-3p's inhibition of eCIRP's pro-inflammation

After increasing the concentration of miRNA 130b-3p from 10 to 1,000 nM, there was a dramatic reduction in the expression of

TNF- $\alpha$  and IL-6 at their protein levels by 45 and 81%, respectively, in the culture supernatants compared to rmCIRP-treated RAW264.7 cells alone (Fig 4A and B). Similarly, with primary murine peritoneal macrophages, treatment of rmCIRP with 1,000 nM of miRNA 130b-3p mimic significantly inhibited rmCIRP alone effects on the protein production of TNF- $\alpha$  in the culture supernatants by 92% (Fig 4C). We extended the list of the inflammatory readouts by performing a multiplex ELISA array on the culture supernatants of the primary peritoneal macrophages treated with rmCIRP in the presence or absence of miR130b-3p mimic. We found that miRNA 130b-3p mimic attenuated the release of a wide range of inflammatory and pleiotropic cytokines including IL-6, G-CSF, GM-CSF, MCP-1, MIP-1 $\alpha$ , RANTES, and IL-17A by the rmCIRP-treated macrophages (Fig EV3). Thus, miRNA 130b-3p attenuates eCIRP's pro-inflammatory effects on murine macrophages.

#### miRNA 130b-3p mimic protects animals from rmCIRP-induced systemic inflammation, lung inflammation, and acute lung injury

We assessed injury markers [aspartate aminotransferase (AST) and lactate dehydrogenase (LDH)] and pro-inflammatory cytokine IL-6 after injecting rmCIRP with or without miRNA 130b-3p mimic into mice. We found that rmCIRP injection into mice significantly increased the serum levels of AST, LDH, and IL-6 (Fig 5A–C). When compared to rmCIRP alone injected mice, the mice injected with rmCIRP and miRNA 130b-3p mimic together had significantly decreased levels of AST, LDH, and IL-6 by mean values of 25, 28, and 62%, respectively (Fig 5A–C). To confirm whether or not this miRNA mimic-dependent inhibition of eCIRP-induced inflammation was specific to the treatment with miRNA 130b-3p mimic, we also injected mice with rmCIRP alone or with miRNA 140 mimic. Surprisingly, treatment with rmCIRP combined with miRNA 140 mimic did not reduce rmCIRP-induced elevated levels of serum AST, LDH, and IL-6 in mice (Table EV4). We also assessed the expression of IL-6 and chemokines like macrophage inflammatory protein-2 (MIP-2) and keratinocyte chemoattractant (KC) in the lung tissues after administration of rmCIRP with and without miRNA 130b-3p mimic. The expression of IL-6, MIP-2, and KC was upregulated following treatment of mice with rmCIRP alone (Fig 5D–F). By contrast, the co-treatment of mice with rmCIRP and miRNA 130b-3p mimic significantly decreased the expression of IL-6, MIP-2, and KC by mean values of 47, 50, and 45%, respectively, when compared to rmCIRP alone (Fig 5D–F). Thus, miRNA 130b-3p suppresses eCIRP's pro-inflammatory effects in mice. It has previously been proven that mice injected with rmCIRP *i.v.* develop ALI [7]. The PBS-treated mice showed normal lung architecture (Fig 5G). The rmCIRP-injected mice developed ALI as evidenced by the presence of hyaline membranes, proteinaceous debris in the alveoli, neutrophils in the alveolar space, neutrophils in the interstitial space, and alveolar septal wall thickening (Fig 5G). There was a significantly increased lung injury score with rmCIRP alone compared to PBS-treated mice (Fig 5H). On the other hand, mice co-injected with rmCIRP and miRNA 130b-3p mimic had a significantly decreased lung injury score by 28% compared to rmCIRP alone mice (Fig 5H). Therefore, treatment of miRNA 130b-3p mimic protects mice from rmCIRP-induced ALI.

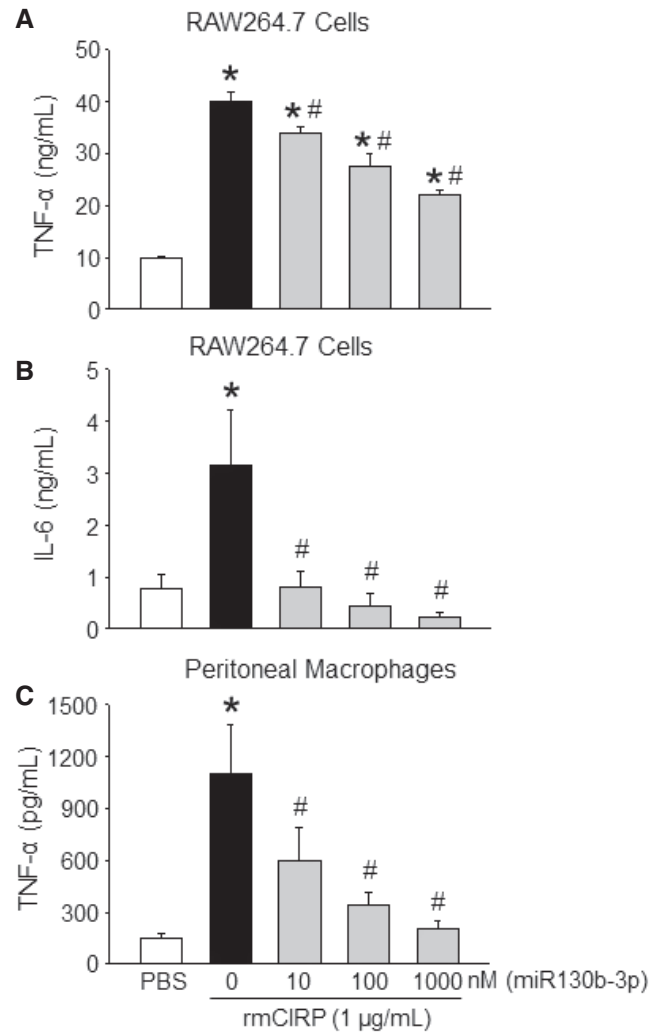


**Figure 4. MicroRNA 130b-3p attenuates eCIRP-induced pro-inflammatory responses in macrophages *in vitro*.**

A, B RAW264.7 cells ( $1 \times 10^6$  cells/ml) were treated with PBS or rmCIRP (1  $\mu$ g/ml) with various doses (10, 100, and 1,000 nM) of miRNA 130b-3p mimic. After 24 h of stimulation, supernatants were collected and assessed for TNF- $\alpha$  and IL-6 by ELISA.

C A total of  $1 \times 10^6$  cells/ml of peritoneal macrophages were treated with PBS or rmCIRP (1  $\mu$ g/ml) with various doses (10, 100, and 1,000 nM) of miRNA 130b-3p mimic. After 24 h of stimulation, supernatants were collected and assessed for TNF- $\alpha$  by ELISA. rmCIRP and miRNAs mimics were combined 30 min prior to stimulation to macrophage cells.

Data information: Data are expressed as means  $\pm$  SE ( $n = 4-6$  samples in each group) and compared by using one-way ANOVA and SNK method (\* $P < 0.05$  vs. PBS; # $P < 0.05$  vs. rmCIRP treatment).

#### miRNA 130b-3p mimic protects mice from polymicrobial sepsis

We next evaluated the efficacy of miRNA 130b-3p mimic in a clinically relevant model of sepsis as induced by cecal ligation and puncture (CLP). We injected miR130b-3p mimic at 2, 5, and 10 h after CLP via intraperitoneal injection (Fig 6A). Three consecutive doses were given to maintain adequate blood levels of miR130b-3p mimic. We choose post-treatment of miR130b-3p mimic in order to provide time for eCIRP to be enriched in the

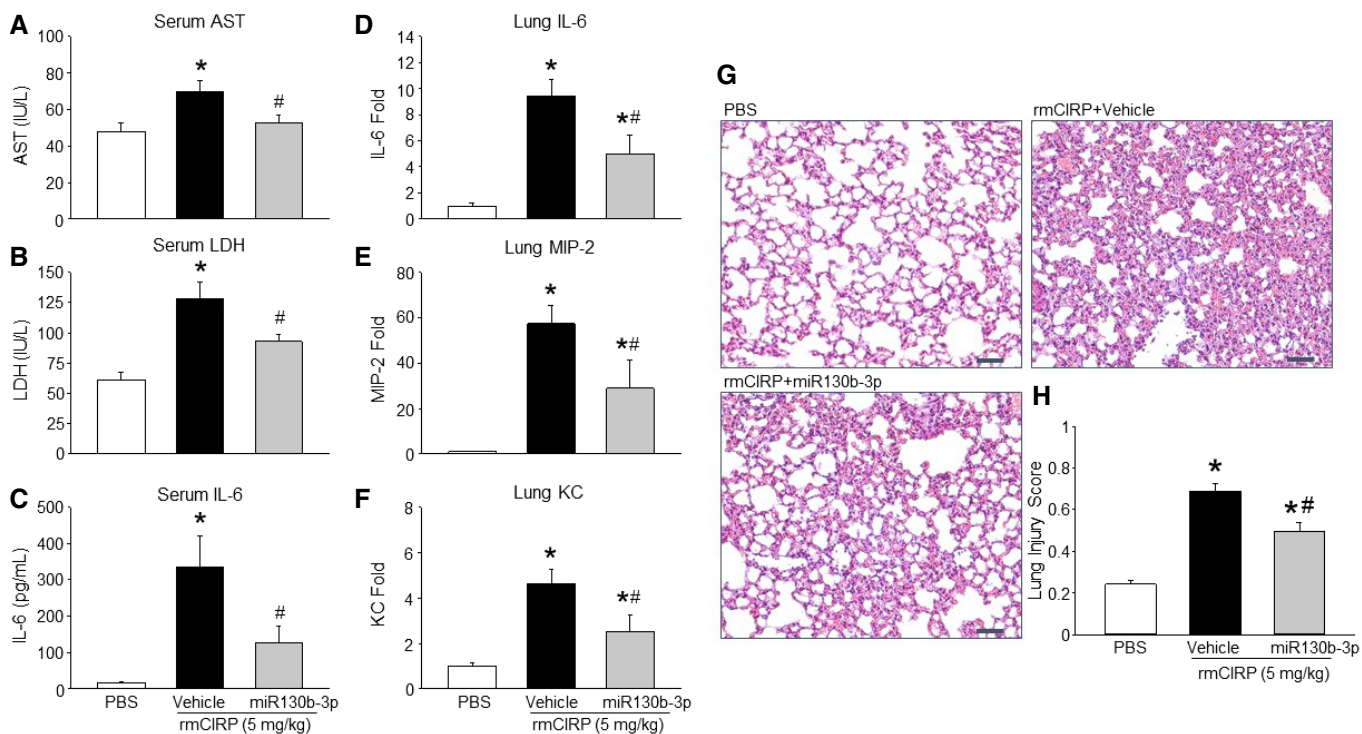


**Figure 5. Treatment of mice with miRNA 130b-3p mimics attenuates eCIRP-induced pro-inflammatory responses and improves overall lung histology.**

Mice were injected with PBS or rmCIRP (5 mg/kg BW) *i.v.* together with or without miRNA 130b-3p at a dose of 12.5  $\mu$ l of 1,000  $\mu$ M. In the miRNA 130b-3p treatment group, rmCIRP and miRNA 130b-3p mimics were combined 30 min prior to administration into mice intravenously.

A–F After 5 h of rmCIRP or miRNA 130b-3p injection into mice, blood samples and lung tissues were collected to assess (A) AST, (B) LDH, (C) and IL-6 in serum and mRNA for (D) IL-6, (E) MIP-2, and (F) KC in the lungs. AST, aspartate aminotransferase; LDH, lactate dehydrogenase; MIP-2, macrophage inflammatory protein-2; KC, keratinocyte chemoattractant.

G Lung tissue was collected after 5 h from PBS- and rmCIRP (5 mg/kg BW)-treated mice with or without miRNA 130b-3p mimic (12.5  $\mu$ l of 1,000  $\mu$ M) and stained with H&E. Each slide was observed under light microscopy at 400 $\times$  original magnification. Representative images for each group are shown. Scale bar, 50  $\mu$ m.

H Histological injury scores of the lungs in different groups were quantified as described in Materials and Methods.

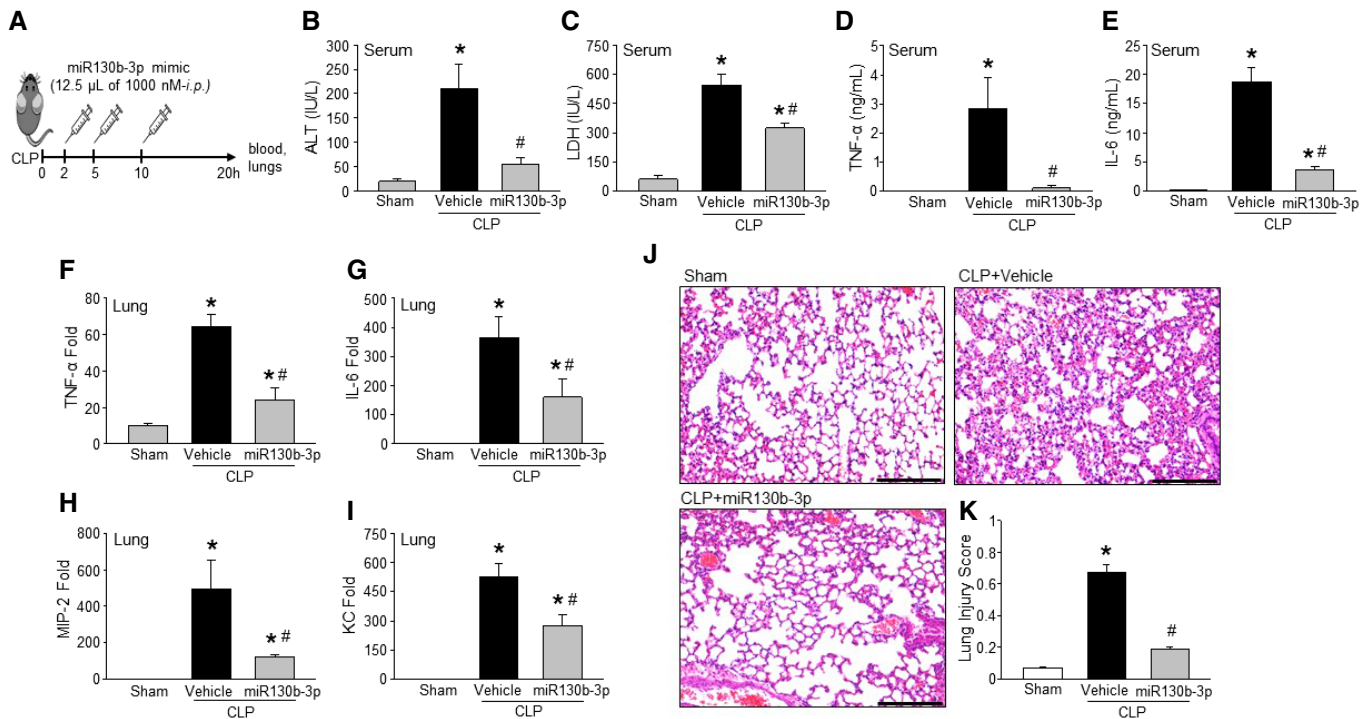
Data information: Data are expressed as means  $\pm$  SE (A–F:  $n = 5$ –8 mice/group; H:  $n = 15$  HPF/group) and compared by one-way ANOVA and SNK method (\* $P < 0.05$  vs. PBS-treated mice; # $P < 0.05$  vs. rmCIRP-treated mice).

serum after sepsis, allowing miR130b-3p mimic to find its target eCIRP in the circulation. CLP caused robust increases in organ injury markers alanine aminotransferase (ALT) and LDH in the serum, while the miRNA 130b-3p-treated mice showed significant decrease in their levels by 73.3 and 40%, respectively (Fig 6B and C). Similarly, the serum TNF- $\alpha$  and IL-6 were elevated by CLP; however, miR130b-3p treatment significantly reduced these levels by 96 and 80%, respectively (Fig 6D and E). Expression of the pro-inflammatory cytokines TNF- $\alpha$ , IL-6, and chemokines like MIP-2 and KC mRNA in lung tissues was increased in CLP-induced sepsis and was significantly reduced with miRNA 130b-3p mimic treatment by 63, 56, 75, and 47.5%, respectively (Fig 6F–I). Histological images of lung tissue in CLP mice displayed significant damage, with increased levels of alveolar congestion, proteinaceous debris, interstitial and alveolar neutrophil infiltration, intra-alveolar capillary hemorrhages, and damage of epithelial architecture (Fig 6J). Treatment of CLP mice with miR130b-3p dramatically improved these histological injury parameters in septic mice (Fig 6J). These histological changes were reflected in a significant decrease in lung tissue injury score in miR 130b-3p-treated mice compared to vehicle mice (Fig 6K). Therefore, administration of

miR 130b-3p mimic exhibits excellent therapeutic potential against murine polymicrobial sepsis.

#### miRNA 130b-3p mimic blocks the interaction of CIRP to TLR4/MD2 complex

It has previously been shown that eCIRP promotes its pro-inflammatory effects by binding its receptor, the TLR4/MD2 complex [8]. We therefore studied the inhibitory effects of miRNA 130b-3p mimic on rmCIRP's ability to bind to the TLR4/MD2 complex. When TLR4/MD2 complex was fixed to the chip and rmCIRP was the analyte, the  $K_d$  value between the two was  $1.17 \times 10^{-7}$  M (Fig 7A). However, when rmCIRP was pre-incubated with varying concentrations of miRNA 130b-3p mimic, there was a dose-dependent decrease in rmCIRP's binding to TLR4/MD2 complex with an  $IC_{50}$  of  $5.6 \times 10^{-8}$  M (Fig 7B). This is further proven with subsequent Biacore tests that kept miRNA 130b-3p mimic concentrations constant at 50 and 100 nM, while varying concentrations of rmCIRP were injected to determine  $K_d$  values. In the presence of 50 and 100 nM of miRNA 130b-3p mimic, the  $K_d$  values of rmCIRP to TLR4/MD2 complex increased to  $4.2 \times 10^{-7}$  M and  $4.0 \times 10^{-5}$  M,



respectively (Fig 7C–E). Increased  $K_d$  values represent decreased binding affinities. To rule out the possibility of the miRNA 130b-3p mimic binding separately to the TLR4/MD2 complex without rmCIRP, and thereby blocking rmCIRP from its receptor, a BIAcore study was done with miRNA 130b-3p mimic as the analyte alone with the TLR4/MD2 complex fixed to the chip. The study showed there was no binding between miRNA 130b-3p mimic and TLR4/MD2 complex (Fig 7F). Therefore, miRNA 130b-3p binds to rmCIRP directly and decreases its affinity for the TLR4/MD2 complex, which ultimately leads to miRNA 130b-3p's inflammatory inhibitory effects on rmCIRP.

## Discussion

The existence of intact, cell-free miRNAs detected in blood samples has raised several questions as to their extracellular functions. These miRNAs are preserved in circulation and are quantifiable, which supports the potential role as diagnostic or progression biomarkers in various diseases [13,24,25]. Although the presence of various miRNAs in the blood has been identified in various diseases, their specific function in the extracellular environment is not fully understood. Our current study looked into the extracellular effect of

a specific miRNA (i.e., miRNA 130b-3p), and its interaction with a novel DAMP, eCIRP, that is known to exert pro-inflammatory effects via its membrane receptor TLR4/MD2 complex. While our data suggest that endogenous miRNA 130b-3p can bind to eCIRP, and the synthetic miRNA 130b-3p mimic can inhibit the activity of eCIRP *in vivo*, it remains to be demonstrated that the mild increase in miRNA 130b-3p seen in sera feeds back to inhibit eCIRP-driven inflammation. Hence, further studies to determine the optimum increase in the serum levels of miRNA 130b at various time-points of sepsis would be worthwhile to clearly establish the inhibitory effect of extracellular miRNA 130b-3p on eCIRP-induced inflammation.

Since there are numerous miRNAs that have already been discovered, we narrowed our scope of research by screening inflammatory relevant miRNAs using a PCR array analysis. After determining which inflammatory miRNAs had a propensity to become elevated in the blood during sepsis, we then reviewed the literature to decide which miRNAs to continue studying for their potential interaction with eCIRP. miRNAs 130b-3p, 27b, and 140, which were each elevated on our PCR array during sepsis, have all been shown to regulate inflammation, specifically via NF- $\kappa$ B [21–23,26]. Their effects are mainly executed inside the cells, still leaving the question of their roles in the extracellular spaces.

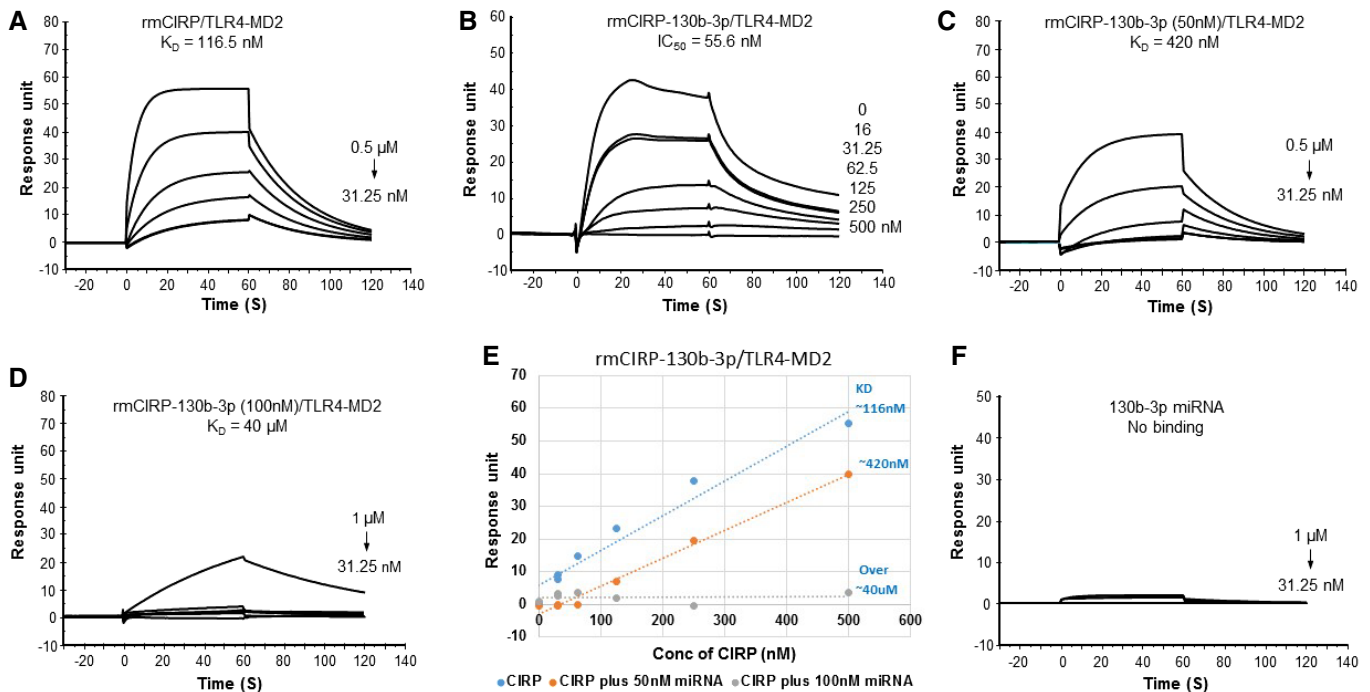


**Figure 7. MicroRNA 130b-3p mimic attenuates rmCIRP's binding to TLR4/MD2 complex.**

Using surface plasmon resonance analysis, TLR4/MD2 complex was immobilized onto a CM5 series chip (GE Healthcare).

- A Varying concentrations of rmCIRP (31.25–500 nM) were injected alone as the analyte ( $K_D$  of  $116.5 \pm 0.8$  nM).
- B  $IC_{50}$  (55 nM) was analyzed by injecting a steady concentration of rmCIRP (0.25  $\mu$ M) combined with varying concentrations of miRNA 130b-3p (16–500 nM) over immobilized TLR4/MD2 complex.
- C, D Varying concentrations of rmCIRP (31.25–1,000 nM) with a constant concentration of 50 nM and 100 nM of miRNA 130b-3p were injected as analytes over immobilized TLR4/MD2 complex ( $K_D$  of 420 nM and 40  $\mu$ M, respectively).
- E Experiments (A, C, and D) plotted to compare response units and  $K_D$  values.
- F To determine that miRNA 130b-3p does not bind TLR4/MD2 complex directly, varying concentrations of miRNA 130b-3p (31.25 nM up to 1,000 nM) were injected as the analyte with TLR4/MD2 complex immobilized onto a CM5 series chip. At least three independent Biacore experiments were performed.

MicroRNA 130b-3p has been described in several pathological states, some of which include inflammatory conditions, bladder cancer, hepatocellular cancer, diabetic nephropathy, lung cancer, and lupus [23,26–30]. Most importantly, serum levels of miRNA 130b-3p can be measured and followed [28,29,31,32]. Both increased and decreased levels of miRNA 130b-3p in blood have been associated with diseased states (i.e., hepatocellular carcinoma, nephroblastomas, and tubulointerstitial fibrosis) [31–33]. The relation of inflammation and miRNA 130b-3p has been previously described intracellularly. Its effects have been linked to the NF- $\kappa$ B pathway in hepatocytes [23]. However, no studies have strictly looked at the role miRNA 130b-3p plays in the extracellular environment during inflammation. Our study provides a stepping stone into the novel mechanisms by which extracellular miRNAs exert their effects in the extracellular environment, specifically in relation to suppressing inflammation.

In the current study, we found increased contents of miRNAs 130b-3p, 27b, and 140 in the blood of mice during sepsis. Other studies have previously found these miRNAs to be increased in the blood during other pathological conditions as well [28,34]. We recently identified a new DAMP, eCIRP, which becomes elevated in the blood during sepsis, hemorrhage, and I/R injuries [reviewed in [7]]. Considering eCIRP and miRNAs 130b-3p, 27b, and 140 are all increased in the blood during sepsis, along with the fact that CIRP is an RNA-

binding protein bearing the RNA-binding motif, we set out to determine the interaction between eCIRP and these miRNAs in the extracellular environment. Specifically, we wanted to know whether the interaction of miRNAs with eCIRP could alter the inflammatory function of eCIRP. Our data clearly showed the binding of these miRNAs to rmCIRP with varied affinities. However, miRNA 130b-3p had the strongest binding capability. In order to reveal the functional effects, we treated macrophages with rmCIRP alone and in combination with miRNAs 130b-3p, 27b, or 140. Surprisingly, we noticed that among them, miRNA 130b-3p mimic had a significant inhibitory effect on rmCIRP-mediated macrophage production of the pro-inflammatory cytokine TNF- $\alpha$ . When these miRNAs were added alone with no rmCIRP, there was no increase in inflammatory cytokines, which shows that alone these miRNAs do not activate inflammation.

As the above studies were performed *in vitro*, we wanted to determine the *in vivo* relationship between eCIRP and extracellular miRNA 130b-3p by carrying out a co-immunoprecipitation experiment using serum samples obtained from septic mice. The results showed there was a significant increase in miRNA 130b-3p levels in the co-IP with native form of CIRP Ab vs. the co-IP with denatured CIRP Ab, suggesting that extracellular miRNA 130b-3p is bound to eCIRP in the blood during sepsis. Using a computational virtual modeling tool, we further revealed eCIRP's binding to extracellular miRNA 130b-3p. Thus, our *in vitro* Biacore data, *in vivo* co-IP (pull-



down) findings, and finally the virtual modeling unequivocally proved eCIRP's novel interaction with extracellular miRNA 130b-3p in sepsis. eCIRP has been previously shown to cause inflammation and ALI [7]. Using an *in vivo* sterile inflammation model and a pre-clinical model of murine polymicrobial sepsis, we further deduced that the treatment of miRNA 130b-3p mimic was also effective in mitigating systemic inflammation of eCIRP or non-sterile model of sepsis by measuring injury markers and ALI in mice. Combined, these findings suggest that miRNA 130b-3p is an endogenous inhibitor of eCIRP. Synthetic decoy, oligonucleotides (ODNs), and mimicking responsive elements of potent transcription factors like NF- $\kappa$ B and AP-1 were shown to attenuate inflammation [35]. Since HMGB1 is a DNA-binding protein, strategy utilizing oligos that recognize HMGB1 also attenuate inflammation [36]. Nonetheless, our finding of extracellular miR130b-3p serving as an RNA decoy molecule to attenuate eCIRP's inflammatory action is novel because of the fact that we discovered this endogenous inhibitor (extracellular miR130b-3p) of eCIRP in an unbiased fashion by performing a hypothesis generating serum miRNA PCR array study.

To identify the mechanism by which miRNA 130b-3p inhibited eCIRP's inflammatory effects, we focused on the interaction of eCIRP with its receptor, TLR4/MD2 complex. A series of BIAcore experiments were completed which revealed miRNA 130b-3p mimic impeded the binding between rmCIRP and TLR4/MD2 complex, which possibly in turn leads to a decreased activation of the pro-inflammatory mediators. At the same time, miRNA 130b-3p mimic does not bind to TLR4/MD2 complex independently, and therefore does not exert inhibitory effects via the TLR4/MD2 pathway by itself. Although BIAcore studies helped us identify the binding abilities between miRNA 130b-3p mimic, rmCIRP, and TLR4/MD2 complex, identification of the CIRP motif where miRNA binds has yet to be discovered. Future studies showing experimental proof of the structural motif of eCIRP bound to the TLR4/MD2 receptor with and without miRNA 130b-3p mimic will be of great interest. Since other DAMPs have multiple receptors, eCIRP may have other unidentified receptors that can lead to activated inflammation. Our current findings may help design future studies that focus on the inhibition of eCIRP when bound to these receptors.

One possible concern when working with miRNA mimics is their stability in the extracellular space. Endogenous miRNAs are stable due to the protection of exosomes or bound proteins [14,15]. The naked miRNA mimics in the extracellular space that are not bound to a protein and not protected in an exosome will only last a few seconds in the blood before being degraded by nucleases [14,15]. Many strategies have been implored to make miRNA mimics stable in the extracellular space. Some of these methods include altering the backbone with peptides creating an achiral structure consisting of N-(2-aminoethyl)-glycine units, creating a 2'-4' methylene bridge, replacing an oxygen with a sulfur, changing the 2'-OH in the ribose ring to 2'-O-methyl, and binding mimics to a nanoparticle [37,38]. Strategies like these will most likely need to be implemented in future studies if naked miRNA mimics are planned to be injected into the extracellular space as a therapeutic inhibitor of inflammation.

Many studies focus on the intracellular function of miRNA. Therefore, the strategy to obtain intracellular miRNA in a functional state is to use double-stranded miRNA mimics and a transfection method [19]. This double-stranded form most closely resembles miRNAs before becoming mature, allowing them to integrate into RISCs [10,11,19]. As

it incorporates itself into RISCs, it becomes single-stranded and exerts its intracellular effects on target mRNAs [11]. However, our study focused on the extracellular effects of already matured single-stranded miRNAs in the extracellular space. Therefore, single-stranded miRNA mimics were used in all aspects of our study.

In the present study, we determined the elevated levels of miR130b-3p in the serum of septic mice as compared to sham mice, regardless of their potential sources or their extracellular forms. miR130b-3p is expressed by various cell types, including epithelial cells, endothelial cells, and macrophages [39–41]. Since cellular apoptosis and necrosis commonly occurs in sepsis, there is a possibility that these cells can release miR130b-3p into the extracellular environment. Extracellular miRNAs can be found in the blood bound by membranes in exosomes and microvesicles, or bound to proteins while membrane-free [42,43]. In the current study, we did not quantify how much of the miRNA 130b-3p is bound by membranes vs. how much is freely circulating in the serum attached to proteins. Theoretically, extracellular miRNAs that are membrane bound will exert their effects intracellularly after merging or being engulfed by the cell. These miRNAs would not be able to interact with eCIRP and the TLR4 receptor which is on the extracellular surface of the cell membrane. However, free protein-bound miRNAs can theoretically exert effects on cell receptors like TLR4. Future studies to determine the free vs. exosome containing miRNAs in the extracellular environment will be informative.

A recent study reported that phosphorothioate ODN can dampen inflammation driven by LPS and HMGB1 [36]. We excluded structural effect of the oligos by pointing to the fact that if the inhibitory effects were based on the chemistry of the backbone alone, and unrelated to the nucleotides, then all three miRNA mimics would have similar inhibitory effects on the rmCIRP-induced inflammation. However, this was not the case and there was a clear difference in the inhibitory effects of the three miRNAs, with miRNA 130b-3p having the strongest inhibition, while one did not have any effect. Also, miRNA 140-5p has the same numbers of nucleotides as miRNA 130b-3p and therefore would have had the same effects if the inhibition was related only to their backbones, since the backbones are identical. Most importantly, the manufacturer uses standard phosphodiester bonds when creating customized RNA sequencing, unless directed otherwise. Our miRNA mimics were single-stranded RNA molecules with backbones that used phosphodiester bonds, thereby excluding phosphorothioate ODN-dependent inhibitory effects.

In conclusion, we demonstrated a novel interaction between miRNA 130b-3p and eCIRP, in which miRNA 130b-3p is an endogenous inhibitor of eCIRP-mediated inflammatory responses, via the TLR4 pathway. This may shed light on miRNA/protein interactions and lead to a new therapeutic strategy in sepsis and other inflammatory diseases.

## Materials and Methods

### Human subjects

Blood samples were obtained from de-identified patients admitted to the Department of Emergency Medicine, North Shore University Hospital, Manhasset, New York. For the control group, blood samples were obtained from the healthy human subjects. Blood

samples were centrifuged at 400 g for 10 min at room temperature, and serum aliquots were stored at  $-80^{\circ}\text{C}$  for the assessment of miRNA 130b-3p and eCIRP by real-time qPCR and ELISA, respectively. Informed consent was obtained from all participants, and human subject protocols were approved by the Institutional Review Board of the North Shore University Hospital.

### Mice

Wild-type male C57BL/6 mice between 8 and 12 weeks of age were purchased from Jackson Laboratories, Bar Harbor, ME. Mice were housed in a temperature-controlled room with 12-h light cycles and fed a standard laboratory chow diet. All animal experiments were conducted in accordance with the National Institutes of Health guidelines for the care and use of laboratory animals, and the protocol was approved by the Institutional Animal Care and Use Committee at the Feinstein Institutes for Medical Research.

### Sepsis model

Sepsis was induced in mice by CLP as described previously [8]. Briefly, mice were anesthetized with 2% isoflurane inhalation. After placing them in the supine position, the abdomen was shaved and wiped with 70% isopropyl alcohol followed by 10% povidone-iodine. A midline laparotomy was performed to expose the peritoneal cavity. The appendix was located and ligated 1 cm from the distal end with a 4-0 silk suture. The blind pouch of the appendix was then punctured through and through once with a 22-gauge needle. At the perforated sites, a small amount of stool was expressed. The abdominal incision was then closed in two layers with 4-0 silk suture. The sham mice underwent anesthesia and a midline laparotomy only with closure. All surgical animals received a 500  $\mu\text{l}$  subcutaneous injection of normal saline for resuscitation. After 20 h, mice were euthanized and blood samples and lung tissues were collected for various analyses.

### Treatment of septic mice with miRNA 130b-3p mimic

Sepsis was induced in mice by CLP. miRNA 130b-3p mimic was injected in mice at the concentration of 125 nM diluted in 100  $\mu\text{l}$  of PBS at 2, 5, and 10 h after CLP via intraperitoneal (i.p.) injection. The sequences of murine single-stranded miRNA mimics are shown in Table EV5. The miRNA 130b-3p mimic was single-stranded RNA molecules with backbones that used phosphodiester bonds synthesized by Integrated DNA Technologies (Coralville, Iowa) and purified by RNase-free HPLC. After 20 h of CLP, we collected blood samples and lung tissue to assess various inflammatory cytokines (TNF- $\alpha$ , IL-6), chemokines (MIP-2, KC), and organ injury markers (ALT, LDH).

### Serum miRNA PCR array and real-time quantitative PCR (qPCR) analysis

Total miRNA was extracted from mouse and human serum using miRNeasy Serum/Plasma Kit (Qiagen, Hilden, Germany). MicroRNA isolation from the serum was controlled for with spike-in of *Caenorhabditis elegans*. cDNA was created using miScript II RT kit (Qiagen). Reverse transcription occurs via creating a polyadenylated tail on the mature miRNAs by poly(A) polymerase with subsequent reverse transcription using oligo-dT primers (Qiagen). We used mouse

Inflammatory Response and Autoimmunity miScript miRNA PCR Array kit purchased from Qiagen (Catalog No.: MIMM-105Z) which has primers of 84 different miRNAs that have been implicated with inflammation. PCR amplification for miRNA PCR array was performed on StepOnePlus real-time machine (Applied Biosystems, Foster City, CA). For confirmation of the expression of selected miRNAs of mouse and human serum, we isolated total miRNA from serum and reverse-transcribed to make cDNA following the above protocol and kits from Qiagen. qPCR amplification was performed on StepOnePlus real-time machine (Applied Biosystems) using mouse miRNA 130b-3p, 27b, and 140 and human miRNA 130b-3p-specific primers (Qiagen). *C. elegans* miRNA 39-3p was spiked in and used to normalize comparative cycle threshold (CT) values. It is worth mentioning that human and mouse miRNA 130b-3p sequences are the same.

### Surface plasmon resonance analysis

BIAcore T200 (GE Healthcare Bio-Sciences, Piscataway, NJ) was used for real-time binding interaction studies. For binding analysis of rmCIRP and miRNA biotinylated single-stranded mimics (Sequence and Integrated DNA Technologies, Skokie, IL), the biotinylated miRNAs 130b-3p, 27b, and 140 were individually immobilized onto separate SA (streptavidin) chips (GE Healthcare). rmCIRP was then sequentially injected at a starting concentration of 500 nM, which was serially diluted to 7.8 nM. The equilibrium dissociation constant ( $K_d$ ) was obtained to evaluate the binding affinity by using the BIAEvaluation 2.0 software (GE Healthcare) supposing a 1:1 binding ratio. For TLR4/MD2 complex and CIRP-binding analyses, human TLR4/MD2 complex (R&D Systems, Cat. No. 3146-TM-050) was immobilized onto a CM5 series chip (GE Healthcare). To evaluate miRNA 130b-3p's inhibition of rmCIRP binding to its receptor, TLR4/MD2 complex, rmCIRP (0.25  $\mu\text{M}$ ) with varying concentrations of miRNA 130b-3p (16–500 nM) was injected over a TLR4/MD2 complex immobilized chip. Varying concentrations of rmCIRP (31.25–1,000 nM) were then incubated with either 50 or 100 nM of miRNA 130b-3p and sequentially injected over a TLR4/MD2 complex immobilized chip to determine  $K_d$  values. The  $K_d$  values were obtained using the BIAEvaluation 2.0 software (GE Healthcare), supposing a 1:1 binding ratio. To evaluate whether there was any independent binding of miRNA 130b-3p to TLR4/MD2 complex, miRNA 130b-3p was sequentially injected with concentrations ranging from 31.25 nM up to 1,000 nM over a TLR4/MD2 complex immobilized chip. Binding experiments were conducted in 1XHBS-EP as the running buffer.

### Co-immunoprecipitation of *in vivo* eCIRP attached to miRNA 130b-3p

Serum was obtained from mice 20 h after CLP or sham operation was performed. A constant volume of serum for each sample was incubated with either commercial CIRP Ab (Proteintech, Rosemont, IL) or denatured CIRP Ab as negative control overnight at  $4^{\circ}\text{C}$ . Denatured CIRP Ab was prepared by heating the commercial CIRP Ab at  $95^{\circ}\text{C}$  for 5 min. Using the Pierce Classic Magnetic IP/Co-IP Kit (Thermo Fisher Scientific), magnetic immunoprecipitation was performed in order to extract eCIRP from the serum, including attached molecules to eCIRP. miRNA was then isolated from the immunoprecipitation using miRNeasy Serum/Plasma Kit (Qiagen). miScript II RT Kit from Qiagen was then used to reverse transcribe cDNA. PCR amplification

was performed on StepOnePlus real-time machine (Applied Biosystems) using miRNA 130b-3p-specific primers (Qiagen). Heparin was not used to collect the blood samples for the quantitative assay of miRNA 130b-3p by qPCR. For serum, *C. elegans* miRNA 39-3p was spiked in and used to normalize comparative CT values.

### Treatment of macrophages with miRNA 130b-3p mimic

Mouse macrophage cell line RAW264.7 cells were purchased from American Type Culture Collection (ATCC) and cultured in Dulbecco's modified Eagle medium (DMEM; Life Technologies Corporation, Grand Island, NY) with 10% of heat-inactivated fetal bovine serum (FBS; MP Biomedicals, Santa Ana, CA), 100 U/ml of each penicillin and streptomycin (Thermo Fisher Scientific, Waltham, MA), and 5% glutamine (Life Technologies Corporation). Prior to experiments, cells were washed with PBS and switched to OPTI-MEM (Life Technologies Corporation) devoid of FBS for a total of 24 h. Cells were treated with 1  $\mu$ g/ml of recombinant mouse (rm) CIRP with or without single-stranded miRNA mimic 130b-3p (Integrated DNA Technologies) at doses of 10, 100, and 1,000 nM. rmCIRP and miRNA mimic 130b-3p were combined 30 min prior to stimulation of RAW264.7 cells. Mouse peritoneal cavity (PerC) macrophages were obtained via peritoneal lavage using 10 ml of PBS with 2% FBS. PerC macrophages were then isolated by centrifugation at 100 g for 10 min and plated for 24 h in a humidified incubator at 37°C with 5% CO<sub>2</sub> atmosphere using RPMI (Roswell Park Memorial Institute) medium (Life Technologies Corporation) with 10% FBS. After 24 h, PerC macrophages were mechanically lifted and plated in RPMI with 1% FBS medium at a concentration of 1  $\times$  10<sup>6</sup> cells/ml. They were treated with either rmCIRP alone, or in combination of rmCIRP with various concentrations of miRNA mimic 130b-3p, which were combined 30 min prior to administration.

### Isolation of mRNA from lungs and real-time qPCR

mRNA was extracted from lung tissues with TRIzol reagent (Invitrogen). Equal amount (3  $\mu$ g) of mRNA was reverse-transcribed into cDNA using reverse transcriptase enzyme (Applied Biosystems). The qPCR was performed from the diluted cDNA templates with forward and reverse primers (Table EV5) and SYBR Green PCR Master Mix (Applied Biosystems) using Applied Biosystems 7300 real-time PCR machine. Mouse  $\beta$ -actin served as an internal control gene for normalization. Relative expression of mRNA was represented as fold change in comparison with the PBS-treated group.

### Induction of inflammation by injecting mice with recombinant mouse CIRP

Mice were injected with rmCIRP (5 mg/kg BW) with either miRNA 130b-3p or normal saline via the internal jugular vein. The rmCIRP was pre-incubated with miRNA 130b-3p (12.5  $\mu$ l of 1,000 nM) for 30 min on ice before injection. Animals were euthanized 5 h later, and blood samples and lung tissues were collected for various analyses.

### Assessment of cytokines and organ injury markers

Serum and cell culture supernatant cytokines TNF- $\alpha$  and IL-6 were measured using mouse enzyme-linked immunosorbent assays (ELISA) kits (BD Biosciences, San Diego, CA). Extracellular CIRP

levels in the human serum were assessed by ELISA (Catalog No.: LS-F25521, LifeSpan Biosciences, Inc, Seattle, WA). Cytokine array was performed from the mouse peritoneal macrophage culture supernatants by using Mouse Cytokine ELISA Plate Array I (Catalog No.: EA-4005, Signosis, Santa Clara, CA). Colorimetric assays were used to measure serum levels of ALT, AST, and LDH using kits from Pointe Scientific, Canton MI.

### Histological lung evaluation

Lung tissues were collected 5 h after injection of rmCIRP or 20 h after CLP with and without treatment with miRNA mimic 130b-3p. Sections of lung were immediately preserved in 10% formalin before permanently fixing in paraffin. Five-micrometer sections of lung tissue were prepared and stained with hematoxylin and eosin (H&E). Light microscopy was used for the evaluation of slides at 400 $\times$  magnification. Histology scoring followed guidelines from the American Thoracic Society Workshop [44]. Scoring focused on the presence of hyaline membranes, the presence of proteinaceous debris in airspaces, alveolar septal wall thickening, and neutrophil infiltration of alveolar and interstitial spaces. Scores were averaged, and each group's mean was compared.

### Virtual modeling

#### Homology modeling of CIRP

We retrieved the sequence of human CIRP from the NCBI database (BAG70039.1). The model was generated using Iterative Threading ASSEmblY Refinement (I-TASSER) server based on templates identified by threading approach to maximize percentage identity, sequence coverage, and confidence [45]. The model of CIRP was generated based on templates, that is, 1X5S (solution structure of RRM domain in A18 hnRNP), 1QM9 (tandem RNA recognition motifs from polypyrimidine tract binding protein), 2KN4 (structure of the RRM domain of SC35), 3S8S (structure of the RRM domain of human SETD1A), 4C7Q (structure of the Nicotiana tabacum GR-RBP1 RRM domain), 4PKD (U1-70k in complex with U1 snRNA stem-loops 1 and U1-a RRM in complex with stem-loop 2), and 2FY1 (A dual mode of RNA recognition by the RBMY protein).

#### Model refinement

The 3D model of CIRP was refined using GalaxyRefine [46]. The refinement process is based on repetitive relaxations by short molecular dynamics simulations for mild (0.6 ps) and aggressive (0.8 ps) relaxations with 4 fs time step after structure perturbations. The refinement of models improved certain parameters, for example, an increase in Rama favored residues and decrease in poor rotamers.

#### 3D modeling of miR130b-3p

We retrieved the sequence of human miRNA 130b-3p (miRBase Id = hsa-mir-130b-3p) from the miRBase database [47]. The 3D model of miRNA 130b-3p was generated using RNAComposer server, which is a method based on machine translation principle and operates on the RNA-FRABASE database [48].

#### Docking studies

The docking of CIRP and miR130b-3p was performed using NPdock [49] that combines GRAMM program to perform a rigid body global

search, ranking, and scoring of best decoys using statistical potentials, clustering of best decoys, and finally, a Monte Carlo simulated annealing procedure (with protein and nucleic acid molecules treated as rigid bodies) to optimize the protein–nucleic acid interactions in the representative clusters.

#### miRNA–protein interaction studies

The analyses of miRNA–protein interactions were performed using PDBePISA [50] and KFC2 [51] servers. Visualization of PPI and miRNA–protein complexes was performed using Chimera [52].

#### CIRP and miR130b-3p interactions

The interaction interface of CIRP and miRNA 130b-3p has a total interface area of 957.1 Å<sup>2</sup>, and the solvation free energy gain upon formation of interface  $\Delta^iG$  is  $-9.8$  kcal/mol. The solvation free energy of assembly dissociation  $\Delta G^{\text{diss}}$  is 4.0 kcal/mol. The rigid body entropy change at dissociation  $T\Delta S^{\text{diss}}$  is 10.7 kcal/mol. The interaction interface of CIRP and miRNA 130b-3p includes Met1, Ile57, Asp58, Lys61, Met64, Asp80, Gln81, Gly83, Lys84, Arg139, Tyr142, Ala143, Ser144, Tyr153, Asp165, His170, Asn171, and Glu172 residues of CIRP and A2, G3, U4, U9, G10, A11, U12, G13, A14, A15, A16, G17, and G18 residues of miRNA 130b-3p. Also, there are 11 hydrogen bonds in the interface of CIRP and miRNA 130b-3p complex. The interface residues involved in hydrogen bond formation in the CIRP, and miRNA 130b-3p complex includes Met1 with U4 (2.66 Å) and G3 (3.87 Å), Lys61 with G3 (2.94 Å) and A2 (3.81 Å), Lys84 with A14 (2.38 Å and 3.74 Å), Ser144 with G18 (3.34 Å), His170 with U12 (3.73 Å), Glu172 with U12 (3.05 Å), Asp165 with A11 (3.49 Å), and Tyr142 with A16 (3.28 Å). These hydrogen bonds are very important for CIRP and miRNA 130b-3p binding.

#### Statistical analysis

Data represented in the figures are expressed as mean  $\pm$  SE. ANOVA was used for one-way comparison among multiple groups, and the significance was determined by the Student–Newman–Keuls (SNK) test. The paired Student's *t*-test was applied for two-group comparisons. Significance was considered for  $P \leq 0.05$  between study groups. Data analyses were carried out using SigmaPlot 12.5 graphing and statistical software (Systat Software, San Jose, CA).

**Expanded View** for this article is available online.

#### Acknowledgements

This study was supported by the National Institutes of Health (NIH) grants R35GM118337 (to P.W.) and R01GM129633 (to M.A.). We thank Alok Jha, Center for Immunology and Inflammation, The Feinstein Institutes for Medical Research (FIMR) for computational virtual modeling, Mian Zhou, and Adnan Arif, Center for Immunology and Inflammation, FIMR for technical assistance.

#### Author contributions

SDG and MA designed the experiments. SDG and HJ performed all the animal and *in vitro* experiments. SDG, MA, and HW performed human studies and analyzed human data. MH and YA-A performed BIAcore studies and BIAcore data analysis. SDG and MA analyzed the data and prepared the figures. SDG and MA wrote the manuscript. JMN, GFC, and PW reviewed and edited the manuscript. PW conceived the idea and supervised the project.

#### Conflict of interest

One of the authors (PW) is an inventor of patent applications covering the fundamental concept of targeting CIRP for the treatment of inflammatory diseases, licensed by TheraSource LLC. PW is a co-founder of TheraSource LLC. Other authors declared that they have no competing interests.

#### References

- Bianchi ME (2007) DAMPs, PAMPs and alarmins: all we need to know about danger. *J Leukoc Biol* 81: 1–5
- Aziz M, Jacob A, Yang WL, Matsuda A, Wang P (2013) Current trends in inflammatory and immunomodulatory mediators in sepsis. *J Leukoc Biol* 93: 329–342
- Garg AD, Galluzzi L, Apetoh L, Baert T, Birge RB, Bravo-San Pedro JM, Breckpot K, Brough D, Chaurio R, Cirone M *et al* (2015) Molecular and translational classifications of DAMPs in immunogenic cell death. *Front Immunol* 6: 588
- Xiang M, Fan J (2010) Pattern recognition receptor-dependent mechanisms of acute lung injury. *Mol Med* 16: 69–82
- Kawasaki T, Kawai T (2014) Toll-like receptor signaling pathways. *Front Immunol* 5: 461
- Nishiyama H, Higashitsuji H, Yokoi H, Itoh K, Danno S, Matsuda T, Fujita J (1997) Cloning and characterization of human CIRP (cold-inducible RNA-binding protein) cDNA and chromosomal assignment of the gene. *Gene* 204: 115–120
- Aziz M, Brenner M, Wang P (2019) Extracellular CIRP (eCIRP) and inflammation. *J Leukoc Biol* 106: 133–146
- Qiang X, Yang WL, Wu R, Zhou M, Jacob A, Dong W, Kuncewitch M, Ji Y, Yang H, Wang H *et al* (2013) Cold-inducible RNA-binding protein (CIRP) triggers inflammatory responses in hemorrhagic shock and sepsis. *Nat Med* 19: 1489–1495
- Brochu C, Cabrita MA, Melanson BD, Hamill JD, Lau R, Pratt MA, McKay BC (2013) NF- $\kappa$ B-dependent role for cold-inducible RNA binding protein in regulating interleukin 1 $\beta$ . *PLoS ONE* 8: e57426
- Carthew RW, Sontheimer EJ (2009) Origins and mechanisms of miRNAs and siRNAs. *Cell* 136: 642–655
- Ha M, Kim VN (2014) Regulation of microRNA biogenesis. *Nat Rev Mol Cell Biol* 15: 509–524
- Gebert LFR, MacRae IJ (2019) Regulation of microRNA function in animals. *Nat Rev Mol Cell Biol* 20: 21–37
- Turchinovich A, Weiz L, Langheinz A, Burwinkel B (2011) Characterization of extracellular circulating microRNA. *Nucleic Acids Res* 39: 7223–7233
- Mitchell PS, Parkin RK, Kroh EM, Fritz BR, Wyman SK, Pogosova-Agadjanyan EL, Peterson A, Noteboom J, O'Briant KC, Allen A *et al* (2008) Circulating microRNAs as stable blood-based markers for cancer detection. *Proc Natl Acad Sci USA* 105: 10513–10518
- Gilad S, Meiri E, Yagev Y, Benjamin S, Lebanony D, Yerushalmi N, Benjamin H, Kushnir M, Cholakh H, Melamed N *et al* (2008) Serum microRNAs are promising novel biomarkers. *PLoS ONE* 3: e3148
- Punga AR, Punga T (2018) Circulating microRNAs as potential biomarkers in myasthenia gravis patients. *Ann N Y Acad Sci* 1412: 33–40
- Correia CN, Nalpas NC, McLoughlin KE, Browne JA, Gordon SV, MacHugh DE, Shaughnessy RG (2017) Circulating microRNAs as potential biomarkers of infectious disease. *Front Immunol* 8: 118
- Hamam R, Hamam D, Alsaleh KA, Kassem M, Zaher W, Alfayez M, Aldahmash A, Alajez NM (2017) Circulating microRNAs in breast cancer: novel diagnostic and prognostic biomarkers. *Cell Death Dis* 8: e3045

19. Feng Y, Zou L, Yan D, Chen H, Xu G, Jian W, Cui P, Chao W (2017) Extracellular microRNAs induce potent innate immune responses via TLR7/MyD88-dependent mechanisms. *J Immunol* 199: 2106–2117
20. Nishiyama H, Itoh K, Kaneko Y, Kishishita M, Yoshida O, Fujita J (1997) A glycine-rich RNA-binding protein mediating cold-inducible suppression of mammalian cell growth. *J Cell Biol* 137: 899–908
21. Lee JJ, Drakaki A, Iliopoulos D, Struhl K (2012) MiR-27b targets PPAR $\gamma$  to inhibit growth, tumor progression and the inflammatory response in neuroblastoma cells. *Oncogene* 31: 3818–3825
22. Karlsen TA, de Souza GA, Ødegaard B, Engebretsen L, Brinchmann JE (2016) microRNA-140 inhibits inflammation and stimulates chondrogenesis in a model of interleukin 1 $\beta$ -induced osteoarthritis. *Mol Ther Nucleic Acids* 5: e373
23. Zheng H, Dong X, Liu N, Xia W, Zhou L, Chen X, Yang Z (2016) Regulation and mechanism of mouse miR-130a/b in metabolism-related inflammation. *Int J Biochem Cell Biol* 74: 72–83
24. Cheng G (2015) Circulating miRNAs: roles in cancer diagnosis, prognosis and therapy. *Adv Drug Deliv Rev* 81: 75–93
25. Wu SC, Yang JC, Rau CS, Chen YC, Lu TH, Lin MW, Tzeng SL, Wu YC, Wu CJ, Hsieh CH (2013) Profiling circulating microRNA expression in experimental sepsis using cecal ligation and puncture. *PLoS ONE* 8: e77936
26. Cui X, Kong C, Zhu Y, Zeng Y, Zhang Z, Liu X, Zhan B, Piao C, Jiang Z (2016) miR-130b, an onco-miRNA in bladder cancer, is directly regulated by NF- $\kappa$ B and sustains NF- $\kappa$ B activation by decreasing Cyclindromatosis expression. *Oncotarget* 7: 48547–48561
27. Wang WY, Zhang HF, Wang L, Ma YP, Gao F, Zhang SJ, Wang LC (2014) High expression of microRNA-130b correlates with poor prognosis of patients with hepatocellular carcinoma. *Diagn Pathol* 9: 160
28. Wang W, Mou S, Wang L, Zhang M, Shao X, Fang W, Lu R, Qi C, Fan Z, Cao Q et al (2015) Up-regulation of serum miR-130b-3p level is associated with renal damage in early lupus nephritis. *Sci Rep* 5: 12644
29. Lv C, Zhou YH, Wu C, Shao Y, Lu CL, Wang QY (2015) The changes in miR-130b levels in human serum and the correlation with the severity of diabetic nephropathy. *Diabetes Metab Res Rev* 31: 717–724
30. Colangelo T, Fucci A, Votino C, Sabatino L, Pancione M, Laudanna C, Binaschi M, Bigioni M, Maggi CA, Parente D et al (2013) MicroRNA-130b promotes tumor development and is associated with poor prognosis in colorectal cancer. *Neoplasia* 15: 1086–1099
31. Ludwig N, Nourkami-Tutdibi N, Backes C, Lenhof HP, Graf N, Keller A, Meese E (2015) Circulating serum miRNAs as potential biomarkers for nephroblastoma. *Pediatr Blood Cancer* 62: 1360–1367
32. Hu XY, Li L, Wu HT, Liu Y, Wang BD, Tang Y (2018) Serum miR-130b level, an ideal marker for monitoring the recurrence and prognosis of primary hepatocellular carcinoma after radiofrequency ablation treatment. *Pathol Res Pract* 214: 1655–1660
33. Bai X, Geng J, Zhou Z, Tian J, Li X (2016) MicroRNA-130b improves renal tubulointerstitial fibrosis via repression of Snail-induced epithelial-mesenchymal transition in diabetic nephropathy. *Sci Rep* 6: 20475
34. Dolz S, Górriz D, Tembl JJ, Sánchez D, Fortea G, Parkhutik V, Lago A (2017) Circulating microRNAs as novel biomarkers of stenosis progression in asymptomatic carotid stenosis. *Stroke* 48: 10–16
35. Tak PP, Firestein GS (2001) NF-kappaB: a key role in inflammatory diseases. *J Clin Invest* 107: 7–11
36. Yanai H, Chiba S, Ban T, Nakaima Y, Onoe T, Honda K, Ohdan H, Taniguchi T (2011) Suppression of immune responses by nonimmunogenic oligodeoxynucleotides with high affinity for high-mobility group box proteins (HMGBs). *Proc Natl Acad Sci USA* 108: 11542–11547
37. van Rooij E, Kauppinen S (2014) Development of microRNA therapeutics is coming of age. *EMBO Mol Med* 6: 851–864
38. Chistiakov DA, Sobenin IA, Orekhov AN (2012) Strategies to deliver microRNAs as potential therapeutics in the treatment of cardiovascular pathology. *Drug Deliv* 19: 392–405
39. Miao Y, Zheng W, Li N, Su Z, Zhao L, Zhou H, Jia L (2017) MicroRNA-130b targets PTEN to mediate drug resistance and proliferation of breast cancer cells via the PI3K/Akt signaling pathway. *Sci Rep* 7: 41942
40. Li S, Geng J, Xu X, Huang X, Leng D, Jiang D, Liang J, Wang C, Dai H (2016) miR-130b-3p modulates epithelial-mesenchymal crosstalk in lung fibrosis by targeting IGF-1. *PLoS ONE* 11: e0150418
41. Wei Y, Zhu M, Schober A (2018) Macrophage microRNAs as therapeutic targets for atherosclerosis, metabolic syndrome, and cancer. *Int J Mol Sci* 19: 1756
42. Turchinovich A, Tonevitsky AG, Burwinkel B (2016) Extracellular miRNA: a collision of two paradigms. *Trends Biochem Sci* 41: 883–892
43. Chen X, Liang H, Zhang J, Zen K, Zhang CY (2012) Secreted microRNAs: a new form of intercellular communication. *Trends Cell Biol* 22: 125–132
44. Matute-Bello G, Downey G, Moore BB, Groshong SD, Matthay MA, Slutsky AS, Kuebler WM; ALIAS Group (2011) An official American Thoracic Society workshop report: features and measurements of experimental acute lung injury in animals. *Am J Respir Cell Mol Biol* 44: 725–738
45. Yang J, Yan R, Roy A, Xu D, Poisson J, Zhang Y (2015) The I-TASSER Suite: protein structure and function prediction. *Nat Methods* 12: 7–8
46. Heo L, Lee H, Seok C (2016) GalaxyRefineComplex: refinement of protein-protein complex model structures driven by interface repacking. *Sci Rep* 6: 32153
47. Kozomara A, Griffiths-Jones S (2014) miRBase: annotating high confidence microRNAs using deep sequencing data. *Nucleic Acids Res* 42: D68–D73
48. Popenda M, Szachniuk M, Antczak M, Purzycka KJ, Lukasiak P, Bartol N, Blazewicz J, Adamiak RW (2012) Automated 3D structure composition for large RNAs. *Nucleic Acids Res* 40: e112
49. Tuszynska I, Magnus M, Jonak K, Dawson W, Bujnicki JM (2015) NPdock: a web server for protein-nucleic acid docking. *Nucleic Acids Res* 43: W425–W430
50. Krissinel E, Henrick K (2007) Inference of macromolecular assemblies from crystalline state. *J Mol Biol* 372: 774–797
51. Darnell SJ, LeGault L, Mitchell JC (2008) KFC Server: interactive forecasting of protein interaction hot spots. *Nucleic Acids Res* 36: W265–W269
52. Pettersen EF, Goddard TD, Huang CC, Couch GS, Greenblatt DM, Meng EC, Ferrin TE (2004) UCSF Chimera—a visualization system for exploratory research and analysis. *J Comput Chem* 25: 1605–1612



**License:** This is an open access article under the terms of the Creative Commons Attribution 4.0 License, which permits use, distribution and reproduction in any medium, provided the original work is properly cited.